α decay of the new isotopes ^{193,194}Rn

A. N. Andreyev,[1,9] S. Antalic,[2] M. Huyse,[3] P. Van Duppen,[3] D. Ackermann,[4,10] L. Bianco,[5] D. M. Cullen,[6] I. G. Darby,[5] S. Franchoo,[7] S. Heinz,[4] F. P. Heßberger,[4] S. Hofmann,[4,11] I. Kojouharov,[4] B. Kindler,[4] A.-P. Leppänen,[8] B. Lommel,[4] R. Mann,[4] G. Münzenberg,[4,10] J. Pakarinen,[5] R. D. Page,[5] J. J. Ressler,[9] S. Saro,[2] B. Streicher,[2] B. Sulignano,[4] J. Thomson,[5] and R. Wyss[12]

[1]*Department of Chemistry, Simon Fraser University, Burnaby, British Columbia, Canada V5A-1S6*
[2]*Department of Nuclear Physics and Biophysics, Comenius University, Bratislava, SK-84248, Slovakia*
[3]*Instituut voor Kern- en Stralingsfysica, University of Leuven, B-3001 Leuven, Belgium*
[4]*Gesellschaft für Schwerionenforschung, Planckstrasse 1, D-64291 Darmstadt, Germany*
[5]*Department of Physics, Oliver Lodge Laboratory, University of Liverpool, Liverpool L69 7ZE, United Kingdom*
[6]*Department of Physics and Astronomy, University of Manchester, Manchester, M13 9PL, United Kingdom*
[7]*IPN Orsay, F-91406 Orsay Cedex France*
[8]*JYFL, Survontie 9, 40014 University of Jyvaskyla, Finland*
[9]*TRIUMF, 4004 Wesbrook Mall, Vancouver, British Columbia, Canada V6T 2A3*
[10]*Institut für Physik, Johannes Gutenberg-University, D–55099 Mainz, Germany*
[11]*Physikalisches Institut, J.W. Goethe-Universität, D–60054 Frankfurt, Germany*
[12]*Department of Physics, Royal Institute of Technology, 104 05 Stockholm, Sweden*

(Received 2 October 2006; published 6 December 2006)

The new neutron-deficient isotopes ^{193,194}Rn have been identified in the complete fusion reaction ^{52}Cr+^{144}Sm $\rightarrow$ ^{196}Rn* at the velocity filter SHIP. The α-decay energy and half-life value of ^{194}Rn were determined to be $E_\alpha = 7700(10)$ keV and $T_{1/2} = 0.78(16)$ ms, respectively. For ^{193}Rn the half-life of $T_{1/2} = 1.15(27)$ ms and two α lines at $E_{\alpha1} = 7685(15)$ keV, $I_{\alpha1} = 74(20)\%$ and $E_{\alpha2} = 7875(20)$ keV, $I_{\alpha2} = 26(12)\%$ were found. The decay pattern of ^{193}Rn, which is substantially different from that of the heavier odd-*A* Rn isotopes, provides first experimental evidence for the long-predicted deformation in the very neutron-deficient Rn nuclei.

DOI: 10.1103/PhysRevC.74.064303 PACS number(s): 23.60.+e, 27.70.+q, 27.80.+w

I. INTRODUCTION

Theoretical calculations have suggested shape coexistence and the onset of permanent strong ground-state deformation in Po and Rn isotopes when approaching the neutron midshell at $N = 104$, see, e.g., Ref. [1]. It is expected that the $^{194-201}$Rn nuclei possess an oblate-deformed ($\beta_2 \sim -0.22$) ground state, whereas a sharp transition to a strongly deformed ($\beta_2 \sim 0.28$) prolate ground state is predicted to happen between ^{194}Rn and ^{193}Rn.

In contrast to theoretical predictions, until now no clear evidence for the onset of the ground-state deformation in the light Rn isotopes could be found experimentally, as exemplified by ^{195,196}Rn [2], being the lightest known Rn isotopes before the present study. However, some of the higher-lying yrast states in the light $^{198-202}$Rn nuclei do show evidence that deformed intruder configuration(s) become important at low excitation energy [3]. Presently, ^{198}Rn is the lightest Rn isotope in which the excited states [up to $I^\pi = (10^+)$] are known [4]. A cross section of $\sigma(^{198}\text{Rn}) \sim 180$ nb was estimated for the complete fusion reaction ^{36}Ar+^{166}Er $\rightarrow$ ^{198}Rn+4n in Ref. [4]. It is instructive to mention that the present limit for traditional in-beam studies is ~50 nb. Combined with rather low beam intensities of up to ~10 pnA, typical for such studies, this practically prohibits the application of the in-beam method for isotopes lighter than ^{198}Rn.

However, α decay provides a powerful complementary tool to investigate very neutron deficient nuclei in the region of $Z \geqslant 82$ and $N \leqslant 126$. One of the main advantages of this method is that the beam intensities up to a few pμA can be used. Combined with efficient, fast, and chemically unselective in-flight recoil separators and modern detection systems that are used at the focal plane, this allows detailed spectroscopic studies at a cross section level down to a few tens of picobarns. By studying the α-decay pattern from nuclei of interest, important conclusions on the configuration of the parent and daughter states can be drawn, see, e.g., Ref. [5] and references therein. As an example, in our recent α-decay studies of the lightest odd-*A* Po isotopes we concluded that a configuration change happens between ^{191}Po and ^{189}Po, the latter isotope possessing a prolately deformed ground state [6], whereas the former has two α-decaying isomeric states, which are due to coexisting oblate and near spherical configurations [7]. Along with the subsequent studies of the new isotopes ^{186,187,188}Po (see Ref. [8] and references therein), these data provided first experimental evidence for the long-predicted island of strong prolate deformation in Po isotopes in the vicinity of and beyond the neutron midshell at $N = 104$.

This work reports on the identification of two new isotopes ^{193,194}Rn. It was performed with a specific goal of extending the chain of Rn isotopes down to ^{193}Rn at which the onset of the strong prolate ground-state deformation is expected.

II. EXPERIMENTAL SETUP

The nuclei ^{193,194}Rn were produced in the complete fusion reaction of ^{52}Cr ions with a ^{144}Sm target. A pulsed ^{52}Cr beam

(5 ms on/15 ms off) with a typical intensity of 500–700 pnA on target was provided by the UNILAC heavy-ion accelerator of the GSI (Darmstadt, Germany). Eight 400-μg/cm^2-thick ^{144}Sm targets were mounted on a target wheel, rotating synchronously with the UNILAC macropulsing. The targets were produced by evaporating $^{144}SmF_3$ material (96.47% enriched) onto a carbon backing of 40 μg/cm^2 thickness and covered with a 10-μg/cm^2-thick carbon layer to increase radiative cooling and reduce the sputtering of the material. Several beam energies in the range of 231–252 MeV in front of the target were used, with the aim to measure at least partially the excitation functions of the nuclei of interest.

After separation by the velocity filter SHIP [9] the evaporation residues (EVRs) were implanted into a 300-μm-thick, 35 $\times$ 80 mm^2 16-strip position-sensitive silicon detector (PSSD), where their subsequent particle decays were measured [10]. The α-energy calibration of the PSSD was performed by using α lines at 6182(4) keV (^{198}Po), 6640.9(25) keV (^{202}Rn), 7167(4) keV (^{192}Po), and 7533(10) keV (^{190}Po) [11–13]. The first three isotopes were abundantly produced in the reactions on the admixtures of the heavier Sm isotopes in the target, whereas the latter isotope was produced in the $\alpha 2n$ channel of the studied reaction. A typical α-energy resolution of each strip of the PSSD was ~20 keV (FWHM) in the energy interval of 6000–8000 keV.

Upstream of the PSSD, six silicon detectors of similar shape (BOX detectors) were mounted in an open box geometry; see details in Ref. [14]. They were used to measure the energies of the particles (α, β, and conversion electrons), escaping from the PSSD in the backward direction. By adding up the energy deposition in the PSSD and BOX detectors, after accounting for the energy loss in the dead layers of both detectors, the full energy of the escaping α particles could be recovered, though with a somewhat reduced energy resolution. A typical α-energy resolution for the sum signal was ~70 keV (FWHM), which was enough in most cases to unambiguously distinguish the decays of interest.

Three thin time-of-flight (TOF) detectors [15] were installed in front of the BOX+PSSD system, allowing us to distinguish the reaction products from the scattered beam particles. More importantly, decay events in the PSSD could be distinguished from the implantation events by requiring an anticoincidence condition between the signals from the PSSD and from at least one of the TOF detectors.

An additional 300-μm-thick silicon detector similar in shape to the PSSD and called further veto detector was installed 8 mm behind the PSSD. It was used to register the energy-loss signals of the high-energy protons and α particles produced in the reactions on the carbon backing of the target and on the carbon charge equilibration foil installed a few cm downstream from the target. Such particles can pass through SHIP undeflected and they are not efficiently registered by the TOF detectors. Therefore, after punching through the PSSD with an energy loss of a few MeV, they create a background in the region of the α particles from the decay of studied nuclei. By requiring an anticoincidence between the signals from the veto and from the PSSD detector, a clear distinction between the decays and punch-through events is established.

A large-volume fourfold segmented Clover germanium detector was installed behind the PSSD for the prompt and delayed EVR-γ and/or α-γ coincidence measurements. Absolute efficiency calibration for this detector is described in Ref. [16].

III. EXPERIMENTAL RESULTS

A. ^{194}Rn

The main data for the new isotope ^{194}Rn were collected at the beam energy of $E(^{52}\mathrm{Cr}) = 236$ MeV in front of the target (232 MeV in the middle of the target). The identification of ^{194}Rn was performed by using time-position correlation of its α decays with the known α decays of daughter isotope ^{190}Po ($E_\alpha = 7533(10)$ keV, $T_{1/2} = 2.45(5)$ ms [12]) and granddaughter nucleus ^{186}Pb ($E_\alpha = 6335(10)$ keV, $T_{1/2} = 4.79$ s [11]; see also Fig. 3).

Figure 1(a) shows a part of the α-particle energy spectrum measured in the PSSD within 5 ms after the recoil implantation. A few α peaks with $E_{\alpha 1} \leqslant 7600$ keV were easily attributed to known nuclei based on their α-decay properties and correlation with respective daughter α decays. In particular, a forthcoming study [17] will discuss the considerably improved data for ^{194}At, produced in the p, $1n$ evaporation channel of the studied reaction.

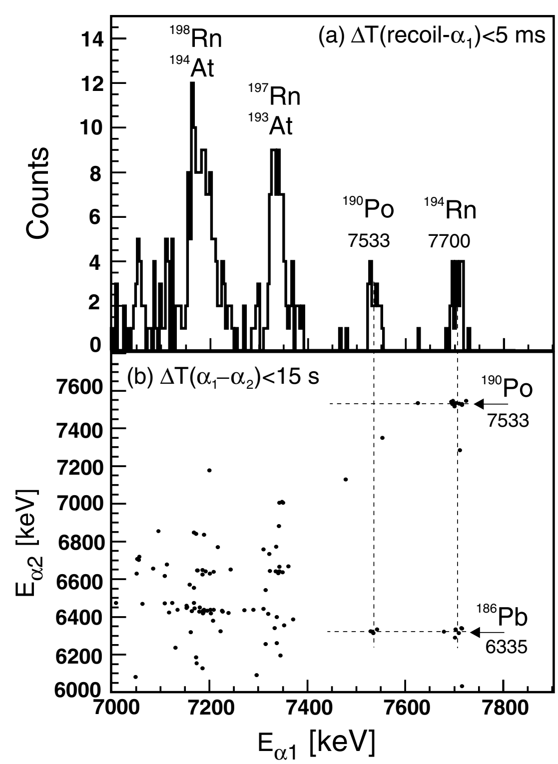

FIG. 1. (a) A part of the α_1-energy spectrum from the reaction ^{52}Cr(236MeV) + ^{144}Sm $\rightarrow$ ^{196}Rn* registered in the PSSD within 5 ms after the recoil implantation. (b) the two-dimensional $E_{\alpha 1}$-$E_{\alpha 2}$ plot for ΔT(recoil-α_1) $\leqslant$ 5 ms and $\Delta T(\alpha_1$-$\alpha_2) \leqslant 15$ s. α-decay energies are given in keV.

The two-dimensional $E_{\alpha 1}$-$E_{\alpha 2}$ correlation spectrum for ΔT(recoil-α_1) $\leqslant 5$ ms and $\Delta T(\alpha_1$-$\alpha_2) \leqslant 15$ s is shown in Fig. 1(b). The latter time interval is equal to three half-lives of ^{186}Pb.

The α peak with 23 counts in Fig. 1(a) at $E_{\alpha 1} = 7700(10)$ keV is in correlation with the daughter decays at $E_{\alpha_2} = 7533(10)$ keV and $E_{\alpha_3} = 6335(10)$ keV [Fig. 1(b)], which correspond to the decay energies of ^{190}Po and ^{186}Pb. The lower number of the $\alpha_1(^{194}$Rn)-$\alpha_3(^{186}$Pb) correlated events in Fig. 1(b) [in comparison with the $\alpha_1(^{194}$Rn)-$\alpha_2(^{190}$Po) events] is due to the α-branching ratio of $b_\alpha(^{186}$Pb) $= 38(9)\%$ [18]. The measured time distributions of the α_2 and α_3 decays are also in agreement with the known half-lives of the respective isotopes. On these grounds, the α decays at $E_{\alpha 1} = 7700(10)$ keV were attributed to the new isotope ^{194}Rn. Three additional full energy recoil-α_1 correlation chains were observed by considering also the escaping α_1 particles, for which the full energy $E_{\alpha 1}(^{194}$Rn) $= 7700(40)$ keV signal could be recovered by adding up the signals from the PSSD and BOX detectors. By using all 26 full-energy correlated recoil-α_1 decays a half-life of $T_{1/2} = 0.78(16)$ ms was deduced for ^{194}Rn.

A search was performed for the fine-structure α decays of ^{194}Rn toward expected low-lying $0^+_{2,3}$ ($E^* \sim 40$–170 keV) excited states in ^{190}Po [19], being the bandheads of the expected spherical and prolate coexisting configurations. Such a decay would have a lower energy and should be in coincidence with x rays and/or conversion electrons, both of them arising from the subsequent internal conversion of the $0^+_{2,3} \rightarrow 0^+_{\text{g.s.}}$ decays in ^{190}Po. Furthermore, such fine-structure decays should be in correlation with the α decays of ^{190}Po and ^{186}Pb. As seen in Fig. 1 the only candidate for such a decay of ^{194}Rn is the single event at $E_{\alpha 1} = 7624$ keV lying between the peaks of ^{190}Po and ^{194}Rn. As it correlates with the α decay of ^{190}Po [Fig. 1(b)] it must originate from ^{194}Rn. However, with only one event of such kind, we can not exclude the possibility that this α_1 decay is an escape event, with most of the energy deposited in the PSSD, whereas the remaining energy of $\sim$80 keV was lost in the dead layers of the PSSD and/or BOX detectors. The decay scheme of ^{194}Rn is shown in Fig. 3 and will be discussed later in the text.

B. ^{193}Rn

The data for the new isotope ^{193}Rn were collected at a single beam energy of $E(^{52}$Cr) $= 252$ MeV in front of the target.

Figure 2(a) shows a part of the α-particle energy spectrum measured in the PSSD within 5 ms after the recoil implantation. The most pronounced α peaks are due to ^{190}Po (α, $2n$ channel) and the complex α decay of ^{193}At ($p, 2n$ channel) [20], which are confirmed by the recoil-α_1-α_2 correlation with their daughter products ^{186}Pb and ^{189}Bi^{m,g}, respectively; see Fig. 2(b). The ΔT(recoil-α_1) $\leqslant 5$ ms and $\Delta T(\alpha_1$-$\alpha_2) \leqslant 18$ s time intervals were used to produce Fig. 2(b). The latter interval is equal to three half-lives of ^{185}Pb.

The broad structure with two weak peaks at 7685(15) keV (nine events) and 7875(20) keV (five events) in Fig. 2(a) is attributed to the decay of the new isotope ^{193}Rn. This is based on the time-position correlations of these decays with

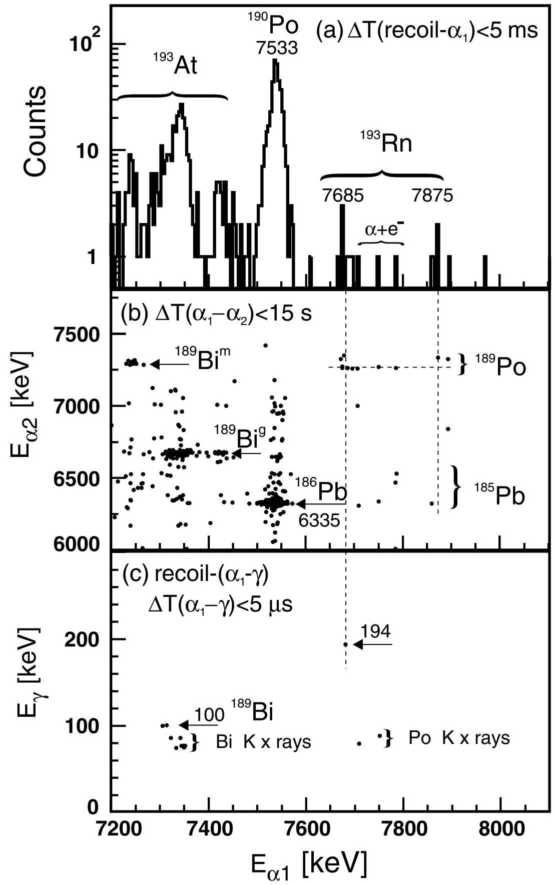

FIG. 2. (a) A part of the α_1-energy spectrum from the reaction ^{52}Cr(252MeV) + ^{144}Sm $\rightarrow$ ^{196}Rn* registered in the PSSD within 5 ms after the recoil implantation. (b) The two-dimensional $E_{\alpha 1}$-$E_{\alpha 2}$ plot for ΔT(recoil-α_1) $\leqslant 5$ ms and $\Delta T(\alpha_1$-$\alpha_2) \leqslant 18$ s. (c) α_1-γ spectrum [$\Delta T(\alpha_1$-$\gamma) \leqslant 5$ μs] for α_1 decays from part a. α- and γ-decay energies are given in keV.

the known α decays of daughter isotopes ^{189}Po and ^{185}Pb; see Figs. 2(b) and 3. Both ^{189}Po and ^{185}Pb isotopes have complex fine-structure α-decay schemes with three α lines in the region of 7259–7532 keV (^{189}Po [6]) and 6288–6548 keV (^{185}Pb, [21]), some of them feeding low-lying excited states in the respective daughter products, ^{185}Pb and ^{181}Hg (see Fig. 3). As an example, the horizontal dashed line in Fig. 2(b) shows the position of the highest-intensity fine-structure 7259-keV decay of ^{189}Po, feeding the excited state at 278 keV in ^{185}Pb. Subsequent deexcitation from this excited state involves conversion electron emission and α-e^- summing in the PSSD, which results in a shift and/or broadening of the measured α peak to higher energies, see detailed discussion in Ref. [6,21]. This effect explains the broader energy distribution of the α decays of ^{189}Po and ^{185}Pb in Fig. 2(b).

Figure 2(c) shows the prompt α-γ coincidence spectrum for the events from Fig. 2(a). We stress that there should be no random events in Fig. 2(c), which is proved by the absence of any coincidences with the 7533-keV α decay of ^{190}Po, being the strongest peak in Fig. 2(a). The group in the lower left corner is due to the α(7325 keV)-γ (99.6 keV) decay of ^{193}At $\rightarrow$ ^{189}Bi observed in Ref. [20]. The

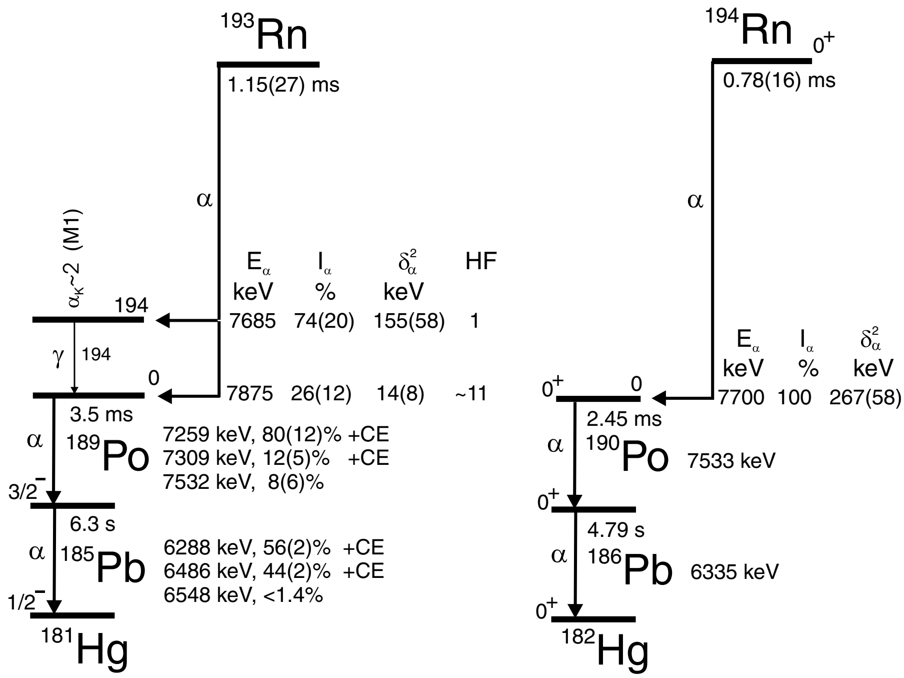

FIG. 3. Decay schemes of new isotopes ^{193,194}Rn. The simplified decay schemes of their daughter products are taken from Refs. [6,12,21]. The label +CE after the α-decay energy and intensity values means that this α decay may be followed by the conversion electron emission; see text for details. The reduced α-decay widths δ_α^2 and hindrance factors HF were calculated with the Rasmussen prescription [22], by assuming $\Delta L = 0$ α decays. The value HF $= 11$ for the 7875-keV decay of ^{193}Rn was calculated relative to the HF value for the 7685-keV decay, for which HF $= 1$ was assumed see text.

three remaining events with $E_{\alpha 1} > 7600$ keV are attributed to the decay of ^{193}Rn as they correlate with the daughter decays of ^{189}Po.

A single α_1(7682 keV)-γ(194 keV) coincident pair is assigned to the decay of ^{193}Rn to the 194-keV excited state in ^{189}Po. This is because the full $Q_{\alpha,\mathrm{full}}$ energy of the α_1(7682 keV)-γ(194 keV) pair $Q_{\alpha,\mathrm{full}} = Q_\alpha$(7682 keV) + E_γ(194 keV) $= 8039(15)$ keV matches well to the $Q_\alpha = 8042(20)$ keV value of the 7875-keV decay in Fig. 2(a). This scenario is also supported by the observation of two α decays with $E_\alpha \sim 7700$–7750 keV in coincidence with the Po K x rays [Fig. 2(c)]. The coincident Po K x rays originate most probably after internal conversion of the 194-keV γ transition. On these grounds, the decay scheme of ^{193}Rn shown in Fig. 3 was constructed.

From the ratio of the observed α_1(^{193}Rn)-Po K x rays events (two events) and α_1(^{193}Rn)-γ(194 keV) events (one decay) in Fig. 2(c), after correction for the corresponding γ-ray efficiencies, the K-conversion coefficient of the 194-keV transition was deduced as $\alpha_K \sim 2$. By comparing the latter value with the theoretical values [23] of $\alpha_K(E1) = 0.07$, $\alpha_K(E2) = 0.18$, $\alpha_K(M1) = 1.46$, $\alpha_K(M2) = 6$, an $M1$ multipolarity was tentatively assigned to the 194-keV transition. The prompt character of the 194-keV transition rules out the higher multipolarities.

The energy of the resulting K-shell conversion electron is $E_e = 194$ keV-$B_e(K) = 101$ keV, where $B_e(K) = 93.1$ keV is the K-shell electron binding energy in Po nuclei [11]. The α(7685 keV)-e^- summing in the PSSD is then responsible for the events between the peaks at 7685 and 7875 keV that are marked by the label $\alpha + e^-$ in Fig. 2.

The half-life of $T_{1/2}$(^{193}Rn) $= 1.15(27)$ ms was deduced from 19 full-energy recoil-α_1(7670 keV-7890 keV) decays, which includes 16 events with the full-energy deposition in the PSSD [Fig. 2(a)] and 3 events in which the energy was shared between the PSSD and BOX detectors.

The α-branching ratio of b_α(^{185}Pb) $= 38(19)$% was deduced by comparing the number of recoil-^{193}Rn-^{189}Po and recoil-^{193}Rn-^{185}Pb correlations in Fig. 2(b). This value is in agreement with but slightly more precise than the value of b_α(^{185}Pb) $= 34(25)$% measured in Ref. [6].

It is worth noting that in the heavier odd-A $^{195-203}$Rn isotopes, two α-decaying isomeric states are known, with rather similar half-lives (typically within a factor of 2) and quite similar α-decay energies (within less than 100 keV). Their distinction was usually performed based on the correlation with the known α decays of the isomeric states in the daughter and granddaughter nuclei. Based on our data we cannot completely rule out the presence of two α-decaying isomeric states in ^{193}Rn that would have quite similar decay energies and half-lives. However, due to low number of observed events and complex decay schemes of the daughter ^{189}Po and granddaughter ^{185}Pb isotopes, we prefer not to speculate on this possibility.

The decay scheme of ^{193}Rn will be discussed later in the text.

C. Production cross section values for ^{193,194}Rn

Maximum production cross sections of ^{193,194}Rn were deduced as σ(^{194}Rn) $= 120(50)$ pb at E(^{52}Cr) $= 232$ MeV in the middle of the target and σ(^{193}Rn) $= 50(20)$ pb at E(^{52}Cr) $= 248$ MeV in the middle of the target. Both values were measured at the beam energies that are expected to correspond to the maxima of the respective excitation functions. Most probably, the $2n$ channel of the ^{52}Cr+^{144}Sm $\rightarrow$ ^{196}Rn* reaction is slightly subbarrier, which explains rather

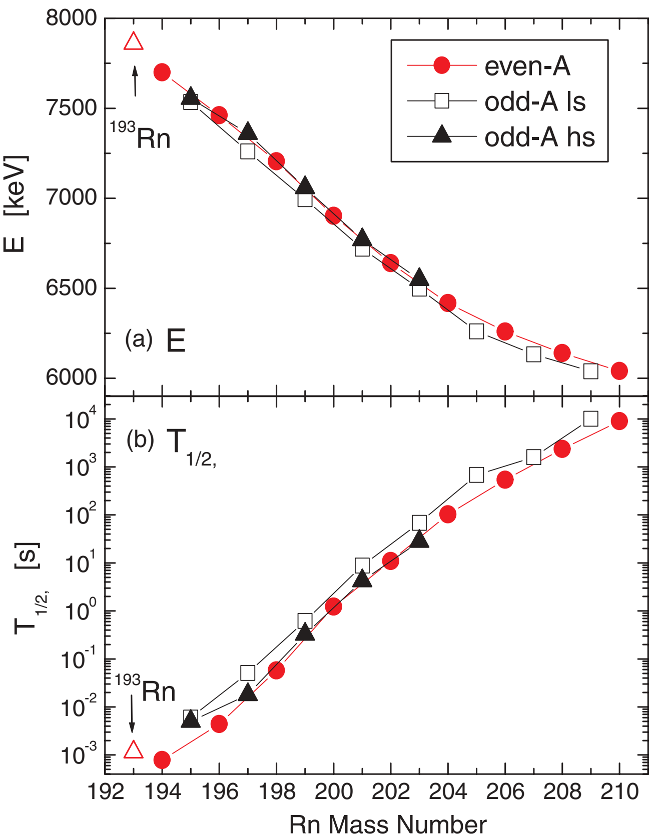

FIG. 4. (Color online) α-decay systematics for the A(Rn)$\leqslant 210$ Rn isotopes: (a) α-decay energies; (b) partial $T_{1/2,\alpha}$ values. For the odd-A isotopes the data for the high-spin $I^{\pi} = 13/2^{+}$ isomers and for the low-spin ground states in $^{195-201}$Rn ($I^{\pi} = 3/2^{-}$) and in $^{203-209}$Rn ($I^{\pi} = 5/2^{-}$) are shown. The spin-parity assignment for ^{193}Rn, shown by the open triangle, was not established in this work.

similar cross section values for the $2n$ and $3n$ evaporation channels.

IV. DISCUSSION

Figures 4(a) and 4(b) show the systematics of the α-decay energies and partial half-lives for the isotopes $^{193-210}$Rn. In the odd-A isotopes in this mass region the spin value is known experimentally only for the low-spin $I^{\pi} = 5/2^{-}$ ground states of ^{205,207,209}Rn and for the high-spin $I^{\pi} = 13/2^{+}$ isomer in ^{203}Rn [24]. For all other α-decaying states in $^{195-203}$Rn the spin-parity assignments are tentative and are based on systematics deduced either from the α- or γ-decay studies. It is generally assumed that the high-spin α-decaying $I^{\pi} = (13/2^{+})$ isomer was observed in $^{195-203}$Rn, whereas the most probable spin-parity value for the low-spin ground states in $^{195-201}$Rn is $I^{\pi} = (3/2^{-})$ and $I^{\pi} = (5/2^{-})$ in ^{203}Rn.

Figures 4(a) and 4(b) demonstrate that the α-decay energies and partial half-lives of the α-decaying states in the odd-A $^{193-209}$Rn isotopes follow well the smooth trend of the $0^{+}_{\mathrm{g.s.}} \to 0^{+}_{\mathrm{g.s.}}$ α decays in their even-A neighbors $^{194-210}$Rn. This is similar to the α-decay properties of the odd-A $^{191-201}$Po isotopes, which follow very closely the decay properties of their even-A neighbors $^{190-200}$Po; see discussion in Ref. [8].

Such a behavior can be interpreted in a simple picture in which the corresponding states in the odd-A Rn and Po nuclei in this mass region are produced by a weak coupling of the valence $3p_{3/2}$, $2f_{5/2}$, or $1i_{13/2}$ neutron to the states in the even-A core. In this approach, the odd neutron is considered as a spectator and is not actively involved in the α-decay process, except for a small correction in the α-particle formation probability due to the blocking effect. The occupation of an orbital at the Fermi surface by an odd particle will reduce the α-particle formation probability as it reduces the pairing correlations. Clearly, the blocking effect will have a larger influence in a smaller shell like $3p_{3/2}$ or $2f_{5/2}$ in comparison with a larger one such as $1i_{13/2}$. This is most probably one of the reasons responsible for systematically longer half-lives of the $3/2^{-}$ and $5/2^{-}$ g.s. in comparison with the $13/2^{+}$ states in $^{195-203}$Rn. This is also similar to the decay properties of the odd-A Po isotopes, in which the α decay from the $3/2^{-}$ ground state has always a longer half-life (with the only exception in ^{191}Po [7]) in comparison with the decay from the $13/2^{+}$ isomer; see discussion in Ref. [8]. This effect is seen more clearly when discussed in terms of reduced α widths δ^{2}_{α} or hindrance factors, in which the energy dependence is removed from the consideration; see details in Ref. [8,25]. Indeed, as shown in Table I of Ref. [25], the α decay between the $3/2^{-}$ states of Po (^{191g,193g,195g}Po) and Pb has a systematically slightly higher hindrance factor (HF ~ 2.5), compared to the decay between the $13/2^{+}$ states (HF $\sim$2). Apart from the slight retardation due to the blocking effect, these decays are considered as unhindered.

The rather uncertain data on the α-decay branching ratios and/or half-lives of the odd-A $^{195-203}$Rn isotopes do not presently allow us to perform a similar comparison for these nuclei. Nevertheless, we note that the observed α decays from the presumably $3/2^{-}$ and $13/2^{+}$ isomeric states in ^{195}Rn have the hindrance factors of HF $= 2.2$ and HF $= 2.1$ [2], respectively, which are similar to the values for the odd-A Po isotopes. Based on this, a conclusion was drawn in Ref. [2] that the α decays of ^{195}Rn^{m,g} connect the states of the same configuration, spin, and parity in the respective mother-daughter decay chains.

A similar hindrance factor of HF $= \delta^{2}_{\alpha}(^{194}$Rn, 7700 keV$)/\delta^{2}_{\alpha}(^{193}$Rn, 7685 keV$) \sim 1.7(7)$ can be deduced for the ratio of the reduced α-decay widths for the presumably unhindered $0^{+}_{\mathrm{g.s.}} \to 0^{+}_{\mathrm{g.s.}}$ 7700 keV decay of ^{194}Rn and for the largest-intensity 7685 keV decay of ^{193}Rn. This can be understood as due to the blocking effect only and therefore we conclude that the 7685-keV decay proceeds between the states of similar configuration, spin, and parity. In contrast to this, the 7875-keV decay is hindered by HF $\sim$11 (see Fig. 3), which is at least a factor of 5 larger than the hindrance factors deduced for ^{195}Rn^{m,g} in Ref. [2]. This points to a different underlying configuration of the α-decaying ground state in ^{189}Po, on one hand, and of the 194-keV excited state in ^{189}Po and of ^{193}Rn itself, on the other hand.

In this sense there should be a change of configuration either between ^{193}Rn and ^{195}Rn, and/or between their respective daughters ^{189}Po and ^{191}Po as the decay patterns of ^{193}Rn, deduced in this work, and of ^{195}Rn studied in Ref. [2] are quite different. As discussed in our recent studies, a change of the ground-state configuration does happen between ^{191}Po and ^{189}Po, the latter isotope having a prolately deformed ground state [6], whereas the former has two coexisting α-decaying isomeric states with oblate and near spherical configurations [7]. However, the question of whether the change of the daughter configuration alone is responsible for the decay pattern change between ^{193}Rn and ^{195}Rn requires further analysis and possibly, a more detailed experimental study of both ^{193,195}Rn and their daughters ^{189,191}Po.

In conclusion, the new neutron-deficient isotopes ^{193,194}Rn were identified in the complete fusion reaction of ^{52}Cr ions with the ^{144}Sm target. Their α-decay energies and partial half-lives follow well the smooth trends of the respective systematics for the α-decaying states in the $^{195-212}$Rn isotopes. However, the decay pattern of ^{193}Rn differs substantially from that of the heavier odd-A $^{195-211}$Rn isotopes, which might indicate the configuration change to the prolately deformed ground state in of ^{193}Rn as expected from the theoretical predictions.

ACKNOWLEDGMENTS

We thank the UNILAC staff for providing the stable and high intensity ^{52}Cr beam. A.N.A. and J.J.R. were partially supported by the NSERC of Canada. This work was supported by EURONS (European Commission contract no. 506065), by the FWO-Vlaanderen and by the Interuniversity Attraction Poles Programme-Belgian State-Federal Office for Scientific, Technical and Cultural Affairs (IAP grant P5/07) and UK EPSRC.

[1] P. Moller, J. R. Nix, W. D. Myers, W. J. Swiatecki, At. Data Nucl. Data Tables **59**, 185 (1995).
[2] H. Kettunen *et al.*, Phys. Rev. C **63**, 044315 (2001).
[3] R. Julin, K. Helariutta, and M. Muikku, J. Phys. G: Nucl. Part. Phys. **27**, R109 (2001).
[4] R. B. E. Taylor *et al.*, Phys. Rev. C **59**, 673 (1999).
[5] P. Van Duppen and M. Huyse, Hyperfine Interact. **129**, 149 (2000); M. Huyse *et al.*, *ibid.* **132**, 141 (2001).
[6] K. Van de Vel *et al.*, Eur. Phys. J. A **24**, 57 (2005).
[7] A. N. Andreyev *et al.*, Phys. Rev. Lett. **82**, 1819 (1999); A. N. Andreyev *et al.*, Phys. Rev. C **66**, 014313 (2002).
[8] A. N. Andreyev *et al.*, Phys. Rev. C **73**, 044324 (2006).
[9] G. Münzenberg *et al.*, Nucl. Instrum. Methods **161**, 65 (1979).
[10] S. Hofmann *et al.*, Z. Phys. A **291**, 53 (1979); S. Hofmann and G. Münzenberg, Rev. Mod. Phys. **72**, 733 (2000).
[11] R. B. Firestone, *Table of Isotopes*, 8th edition (John Wiley and Sons, New York, 1996).
[12] A. N. Andreyev *et al.*, Nature (London), **405**, 430 (2000).
[13] K. Van de Vel *et al.*, Phys. Rev. C, **68**, 054311 (2003).
[14] A. N. Andreyev *et al.*, Nucl. Instrum. Methods A **533**, 409 (2004).
[15] S. Saro *et al.*, Nucl. Instrum. Methods A **381**, 520 (1996).
[16] F. P. Heßberger *et al.*, Eur. Phys. J. A **22**, 417 (2004).
[17] A. N. Andreyev *et al.*, in preparation (2007).
[18] A. N. Andreyev *et al.*, J. Phys. G: Nucl. Part. Phys. **25**, 835 (1999).
[19] K. Van de Vel *et al.*, Eur. Phys. J. A **17**, 167 (2003).
[20] H. Kettunen *et al.*, Eur. Phys. J. A **17**, 537 (2003).
[21] A. N. Andreyev *et al.*, Eur. Phys. J. A **14**, 63 (2002).
[22] J. O. Rasmussen, Phys. Rev. **113**, 1593 (1959).
[23] The program to calculate conversion coefficients. The National Nuclear Data Center (NNDC), http://www.nndc.bnl.gov/nndc/physco/.
[24] E. W. Otten, in *Treatise on Heavy-Ion Science*, edited by D. A. Bromley (Plenum, New York, 1989), Vol. 8, p. 517.
[25] K. Van de Vel *et al.*, Phys. Rev. C, **65**, 064301 (2002).